

8-8-2019

Testing the Robustness of Solution Force Fields for MD Simulations on Gaseous Protein Ions.

Justin H Lee

Katja Pollert

Lars Konermann

Follow this and additional works at: <https://ir.lib.uwo.ca/chempub>



Part of the [Chemistry Commons](#)

Citation of this paper:

Lee, Justin H; Pollert, Katja; and Konermann, Lars, "Testing the Robustness of Solution Force Fields for MD Simulations on Gaseous Protein Ions." (2019). *Chemistry Publications*. 245.
<https://ir.lib.uwo.ca/chempub/245>

**Testing the Robustness of Solution Force Fields for MD
Simulations on Gaseous Protein Ions**

Justin H. Lee, Katja Pollert, and Lars Konermann*

*Department of Chemistry, The University of Western Ontario, London, Ontario,
N6A 5B7, Canada*

* To whom correspondence should be addressed. Telephone: (519) 661-2111 ext. 86313.

Email: konerman@uwo.ca

ABSTRACT: It is believed that electrosprayed proteins and protein complexes can retain solution-like conformations in the gas phase. However, the lack of high resolution structure determination methods for gaseous protein ions implies that their properties remain poorly understood. Many practitioners tackle this difficulty by complementing mass spectrometry-based experiments with molecular dynamics (MD) simulations. It is a potential problem that the standard MD force fields used for this purpose (such as OPLS-AA/L and CHARMM) were optimized for solution conditions. The question whether these force fields produce meaningful gas phase data has received surprisingly little attention. Standard force fields are overpolarized to account for an aqueous environment, *i.e.*, atomic charges and intramolecular dipole moments are ~20% larger than predicted by gas phase *ab initio* methods. Here we examined the implications of this overpolarization by conducting a series of MD simulations on electrosprayed proteins. Force fields were modified via a charge scaling factor (*CSF*), while ensuring that the net protein charge remained unchanged. *CSF* = 0.8 should roughly eliminate water-associated overpolarization. Gas phase CHARMM simulations on myoglobin with *CSF* = 0.8 and with unmodified parameters (*CSF* = 1) yielded similar results, preserving a compact structure that was consistent with ion mobility experiments. Major structural changes caused by weakened charge-dipole and dipole-dipole contacts occurred only when lowering *CSF* to physically unreasonable values (0.5 and 0.1). Similar results were obtained in mobile-proton OPLS-AA/L simulations on the collision-induced dissociation of transthyretin. Our data support the view that gas phase MD simulations with standard (solution) force fields are suitable for modeling gaseous protein ions in a semi-quantitative manner. Although this is welcome news for the mass spectrometry community, it is hoped that dedicated gas phase MD force fields will become available in the near future.

Introduction

Electrospray ionization (ESI) is widely used for transferring proteins and protein complexes from solution into the gas phase for analysis by mass spectrometry (MS).¹ It appears that under properly optimized conditions the resulting $[M + zH]^{z+}$ ions retain solution-like conformations and interactions. The premise of these “native ESI” studies is that measurements on gaseous proteins can reveal insights into solution properties.²⁻⁷ Retention of solution-like conformations *in vacuo* has been attributed to kinetic trapping.⁸⁻¹²

The widespread use of native ESI-MS notwithstanding, it is clear that electrosprayed proteins will change their structures to some extent.¹³⁻¹⁸ Loops and exposed side chains likely reorient toward the protein surface,¹⁹⁻²¹ internal cavities can collapse,²²⁻²⁴ and hydrophobic contacts may not always survive in the absence of water.^{25, 26} Thus, the exact relationship between protein structure in solution and in the gas phase remains incompletely understood.^{11, 21, 27, 28}

The main difficulty associated with studies on electrosprayed proteins is the lack of high resolution structure determination methods in the gas phase.²⁹ This is in contrast to the condensed phase, where X-ray crystallography,³⁰ cryo-electron microscopy,³¹ and nuclear magnetic resonance (NMR) spectroscopy³² yield atomic information. Ion mobility spectrometry (IMS)-derived collision cross sections (Ω) report on the compactness of electrosprayed ions.^{20, 33-35} However, Ω represents just a single number that is compatible with multiple candidate structures for any given protein.^{11, 34, 36-39} Other techniques that provide partial insights into gas phase structures include dissociation studies,^{16, 40-47} infrared spectroscopy,⁴⁸ fluorescence assays,^{14, 49} and H/D exchange methods.^{50, 51}

The aforementioned challenges have prompted many ESI-MS practitioners to complement their experiments with computational modeling. Density functional theory (DFT)⁵²⁻⁵⁶ yields orbitals and ground state geometries. *Ab initio* molecular dynamics (AIMD)

methods simulate nuclear positions as a function of time, using forces from on-the-fly DFT calculations.⁵⁷⁻⁶² Unfortunately, the high computational cost of DFT, AIMD and related approaches^{63, 64} tends to restrict their application to systems comprising a few hundred atoms, and AIMD time windows are typically limited to tens of picoseconds.⁵⁹⁻⁶¹ Thus, most biomolecular systems are out of reach for these high-level modeling techniques.

Proteins and complexes that are commonly studied by native ESI-MS contain thousands of atoms, and the time scale of interest extends to microseconds and beyond.^{2-7, 37, 65, 66} Molecular dynamics (MD) simulations are the only computational technique that is capable of tackling this size and time regime. MD simulations use force fields that contain information on bonded and non-bonded interactions.⁶⁷⁻⁶⁹ Potential gradients derived from these force fields are used to iteratively solve Newton's equations.⁷⁰ MD techniques are widely used for gas phase protein simulations,^{16, 21, 71, 72} and for generating candidate structures for comparison with experimental Ω values.^{11, 18, 22, 28, 34, 36, 37, 73-76}

A potential problem that has received little attention within the gas phase protein community is that commonly used MD force fields were designed for solution simulations. This includes OPLS-AA/L,⁶⁷ AMBER,⁶⁸ and CHARMM⁶⁹, all of which employ parameters that were initially derived from *ab initio* or DFT calculations, followed by empirical fitting of atomic charges and torsional potential energies to match crystallographic and solution NMR data.^{67, 77} Presently there is no MD force field that has been optimized for gaseous proteins. The blind-faith reliance of the gas phase community on solution force fields is surprising, and a critical examination of this issue seems overdue.^{34, 78}

Standard MD force fields are additive,⁶⁷⁻⁶⁹ *i.e.*, they assign static partial charges to each atom (Figure 1).⁷⁹ Polarization effects are implicitly included by designing these charges in a way that molecular dipoles are larger than the corresponding vacuum *ab initio* values. This overpolarization mimics the effects of intra- and intermolecular contacts. The large

dipole moment of surrounding H₂O molecules is the main contributor to the polarization of solutes in water.^{67, 68, 79, 80} However, other contacts play a role as well; for example, formation of backbone $\delta^-N-H^{\delta^+}\dots\delta^-O=C^{\delta^+}$ hydrogen bonds enhances the partial charges of the participating atoms. Overpolarization also applies to water itself; H₂O in the gas phase has a dipole moment of 1.85 D, whereas MD water models have dipole moments of 2.2 - 2.6 D.^{81, 82} Overall, standard force fields overpolarize molecules by ~20%, largely to account for the effects of an aqueous environment.^{67, 68, 79-83} Polarizable models are available but they come at a high computational cost; also, it is unclear if their gas phase performance is superior to standard fixed-charge models.^{34, 79, 80, 84}

The current study examined to what extent the overpolarization of standard force fields affects the results of gas phase protein simulations. For this purpose we scaled down atomic charges throughout the protein, subject to the conservation of overall charge. Two outcomes of such an endeavor might be envisioned. (1) Even small modifications of atomic charges could have dramatic effects on the simulated gas phase behavior. Such a finding would imply that the application of standard (overpolarized) force fields in the gas phase is problematic. (2) Alternatively, one might find that gas phase MD results remain consistent over a relatively wide range of charge values. This second outcome would support the validity of the widely used strategy^{11, 16, 21, 22, 28, 34, 36, 71-76} where solution force fields are applied to gaseous proteins. The data reported here are more aligned with the second outcome. Although reassuring, this finding should not distract from the fact that improved gas phase modeling techniques are urgently needed.

Charge Rescaling Strategy

As outlined above, standard protein force fields are overpolarized compared to vacuum conditions.^{68, 79-83} Reducing the extent of polarization should therefore, in principle, render force fields more suitable for the vacuum. Nonetheless, the aim of this work was *not* to develop improved gas phase MD parameters. Instead, we simply wanted to explore how altered atomic charges affect simulation results. Charge rescaling was performed in a way that preserved the net charge z of $[M + zH]^{z+}$ protein ions, keeping in mind that z is an experimental observable and a key determinant of ion behavior.^{8, 14, 20, 27}

Figure 1 illustrates unmodified OPLS-AA/L atomic charges for a short peptide. The partial charges in each side chain add up to an integer value, i.e., +1 for a protonated basic residue, -1 for a deprotonated acidic residue, and zero for all others. The same applies to C_α appendages of the N- and C-terminal residues. Multiplication of atomic charges by a charge scaling factor $CSF < 1$ lowers dipole moments throughout the protein, such that the extent of polarization can be controlled. For example, $CSF = 0.5$ would transform atomic charges in a backbone segment according to

$$(N^{-0.5} H^{0.3} C_\alpha^{0.14} H^{0.06} C^{0.5} O^{-0.5}) \rightarrow (N^{-0.25} H^{0.15} C_\alpha^{0.07} H^{0.03} C^{0.25} O^{-0.25})$$

By excluding charged side chains and termini from being CSF -modified, it was possible to rescale dipole moments, while preserving the net charge z . For the proteins examined below this exclusion affected roughly 10% of the atoms, i.e., ~90% of the atomic charges were subject to rescaling. All MD simulations were initially performed with unmodified charges ($CSF = 1$). We subsequently tested $CSF = 0.8$ which should approximately compensate for the ~20% overpolarization that is inherent to standard force fields.⁷⁹⁻⁸³ To further investigate the consequences of charge rescaling, we also tested $CSF = 0.5$ and $CSF = 0.1$, although the

dipole moments associated with the latter two values fall outside of the range that can be expected under realistic conditions.^{68, 79-83}

Charge rescaling effects were tested for two force fields. CHARMM⁶⁹ was the first force field to be used for structural investigations of electrosprayed protein ions,^{73, 85} and it has also been applied for modeling protein release from ESI nanodroplets.⁷⁸ The second force field is OPLS-AA/L,⁶⁷ which currently represents the most popular choice for gas phase protein simulations.^{11, 16, 18, 22, 71}

Methods

Mass Spectrometry and Ion Mobility Spectrometry. Holo-Myoglobin (hMb, 17568 Da) and transthyretin (TTR, 55048 Da) were from Sigma (St. Louis, MO). Samples for native ESI were prepared in 10 mM aqueous ammonium acetate (pH 7) at a protein concentration of 10 μ M. Data were acquired on a Synapt HDMS time-of-flight mass spectrometer (Waters, Milford, MA). hMb spectra were recorded with a standard Z-spray ESI source operated at +2.8 kV / 5 μ L min⁻¹. TTR spectra were acquired using nanoESI with gold-coated borosilicate emitters.⁸⁶ Ion transmission settings were kept as gentle as possible (source temperature 25 °C, desolvation temperature 40 °C, sampling cone 5 V, extraction cone 1 V, trap collision energy 2 V, trap DC bias 8-9 V). For collisional activation of TTR, precursor ions were quadrupole-selected and the trap collision voltage (trap CE) was raised. Traveling wave IMS was conducted with N₂ buffer gas. hMb arrival time distributions were converted to He Ω values using a calibrant protein mix.⁸⁶ Similarly, IMS data for TTR were calibrated using various reference complexes.⁶

Gas Phase Simulations. MD runs were performed on graphics processing unit (GPU) accelerated Linux workstations running Gromacs 2016.⁷⁰ Bond distances were constrained, and the integration step was 2 fs. All runs were conducted in vacuum without cutoffs for Lennard Jones or Coulombic interactions.⁷⁸ 1 μ s hMb simulations (~2500 atoms) were performed using CHARMM36⁶⁹ with static protons at 300 K, and with the X-ray coordinates 1wla as starting structure. The 9+ net charge was implemented via judicious choice of the protonation states for titratable sites [N-terminus (NT)^{0/+}, Arg^{0/+}, Lys^{0/+}, His^{0/+}, Asp^{-/0}, Glu^{-/0}, and C-terminus (CT)^{-/0}]. For example, the “11+/2-“ configuration discussed below employed protonation of NT, R31, K45, H48, K50, K77, H97, K102, H116, R139, K145, along with two deprotonated (negatively charged) heme propionates. All other parameters were as described.¹⁹ For each condition three repeats were conducted with different random starting velocities.

MD runs on TTR (~7700 atoms) used the OPLS-AA/L force field,⁶⁷ starting from the 3GRG crystal coordinates. Collision-induced dissociation of TTR was simulated by operating Gromacs⁷⁰ in conjunction with a mobile H⁺ algorithm.⁸⁷ Briefly, the runs were broken down into 20 ps segments. After each segment H⁺ were redistributed over all acidic and basic titratable sites, subject to minimization of an energy term E_{tot} that reflects electrostatic interactions between charged sites as well as proton affinities. An inherent feature of this algorithm is that pairs of basic and acidic moieties can exist either in their charged forms (e.g., R-NH₃⁺ ⁻OOC-R) or as neutrals (R-NH₂ HOOC-R), as governed by the effects of protein structure on E_{tot} .⁸⁷ Gradual heating was implemented by raising the temperature at a rate of 8.33 K ns⁻¹, starting at 350 K.

Charge rescaling was performed using a Fortran program for modifying Gromacs .top and .itp files that contained the force field-defined atomic charges. These charges were multiplied by a user-selected *CSF*, except for atoms belonging to sites that carried a +1 or -1

net charge (NT⁺, Arg⁺, Lys⁺, His⁺, Asp⁻, Glu⁻, CT⁻). The trajectory method in Collidoscope⁸⁸ was used to calculate He Ω values of MD structures.

Results and Discussion

Myoglobin ESI-IMS/MS. hMb is a tightly folded heme-protein complex that represents a standard ESI-MS model system. Native ESI conditions produced 9+ as the most intense charge state (Figure 2A), with a collision cross section of $\Omega = 1780 \text{ \AA}^2$ (Figure 2B). These experimental data are consistent with previous reports,^{89, 90} and they serve as reference against which MD results can be compared.

Static-Proton MD Simulations. Similar to most previous gas phase studies, we initially conducted simulations using static H⁺ which are the default option in MD force fields.⁶⁷⁻⁶⁹ In these runs the protonation states of all titratable sites remain unchanged throughout the entire simulation. Two types of static H⁺ patterns can be distinguished. (1) Positive-only runs place charges on basic sites (NT⁺, Arg⁺, Lys⁺, His⁺), leaving all acidic sites neutral.^{16, 22, 73} (2) Zwitterionic runs involve protonation at basic sites, with deprotonation of acidic moieties (Asp⁻, Glu⁻, CT⁻).^{19, 21} The second option is consistent with gas phase studies that support the presence of zwitterionic motifs in the form of salt bridges.^{41, 48, 63, 91}

We examined charge rescaling effects by conducting static H⁺ simulations on gaseous hMb using CHARMM36.⁶⁹ The charge state was chosen to be 9+, in accordance with the experiments of Figure 2. Two 9+ protonation patterns were tested. One of these was a 11+/2- combination. This pattern resembles a positive-only case, except that the two negatively charged heme propionates had to be compensated (standard force field parametrizations do not include neutral heme). In addition, we tested zwitterionic 9+ hMb using a 31+/22-

pattern. MD runs were performed for 1 μ s, which is significantly longer than the ns regime of most previous gas phase studies.

Runs with unmodified force field parameters ($CSF = 1$) produced gas phase structures that stayed close to the initial X-ray coordinates, both for 11+/2- and for 31+/22-. Minor structural alterations included slight unravelling of the N-terminus (helix A), as well as transitioning of the short helix D into a loop for 11+/2- (Figure 3A, B, F). Very similar structures were obtained for $CSF = 0.8$, with preservation of the overall tertiary fold and retention of helices A-C and E-H (Figure 3C, G). Significant structural changes became apparent for $CSF = 0.5$, where helices started to unravel and tertiary contacts were lost (Figure 3D, H). This trend continued for $CSF = 0.1$ where the native secondary structure had vanished, and the 11+/2- protein was stretched into an elongated shape (Figure 3E). In contrast, 31+/22- hMb stayed relatively compact (Figure 3I). RMSD values relative to the X-ray starting structure for all simulation conditions are provided in the caption of Figure 3.

The 11+/2- simulations with $CSF = 1$ and 0.8 resulted in Ω values that were close to the experimental collision cross section. Significantly larger Ω values were calculated for $CSF = 0.5$ and 0.1 (Figure 2C). 31+/22- simulations with $CSF = 1$ and $CSF = 0.8$ yielded Ω values that were just below the experimental value, while those with $CSF = 0.5 / 0.1$ were slightly elevated (Figure 2D).

In summary, MD simulations on hMb with unmodified CHARMM parameters ($CSF = 1$) largely preserved the native protein structure. Ω values of the simulated proteins agreed well with the experimental collision cross section. Importantly, MD simulations obtained after rescaling of atomic charges, using $CSF = 0.8$, yielded virtually the same results. As noted above, this ~20% rescaling roughly corresponds to removal of the overpolarization that accounts for solvent effects.⁷⁹⁻⁸³ For hMb the use of overpolarized solution parameters thus affects the outcome of gas phase simulations only to a very small degree. Significant effects

were observed only when rescaling atomic charges down to values that fell outside of reasonable physical expectations, *i.e.*, CSF s of 0.5 or 0.1.^{68, 79-83}

Coulombic Repulsion vs. Charge Solvation. Electrostatics are a key determinant of gas phase ion behavior, giving rise to two opposing trends.^{8, 14, 20, 27} The $z > 1$ net charge of electrosprayed proteins is destabilizing and tends to cause Coulombic unfolding. On the other hand, compact structures are favored by packing of cationic/anionic groups, intramolecular charge solvation (charge-dipole interactions), and dipole-dipole contacts.^{19, 41, 92-94} The rescaling performed here illustrates the competition between these two trends, providing an explanation for the dissimilar behavior of the 11+/2- and 31+/22- models. It is instructive to compare the two extreme cases of $CSF = 1$ and $CSF = 0.1$. Once again, it is noted that $CSF = 0.1$ represents an unreasonably low value.^{68, 79-83} We use it here only as a diagnostic tool that magnifies the interplay of stabilizing/destabilizing electrostatic forces.

A major contributor to the retention of native-like structure in 11+/2- hMb for $CSF = 1$ was charge solvation at the protein surface, where protonated basic sites closely interacted with carbonyl oxygens in adjacent neutral side chains and backbone loops. Other electron-rich moieties such as R-H₂N: participated in charge solvation as well (Figure 4A). In addition, the structure was stabilized by H-bonds (modeled as dipole-dipole contacts)⁷⁹ within the eight helices. Overall, the strong polarization of the unmodified force field ensured preservation of a native-like structure in the gas phase because attractive intramolecular contacts dominated over Coulombic repulsion (Figure 3B, 4A).

A different situation was encountered for 11+/2- hMb with $CSF = 0.1$. Dipole-mediated charge solvation was dramatically reduced under these conditions, causing unshielded cationic sites to minimize their mutual repulsion by protruding from the surface. This is illustrated in Figure 4B, where the K102/K145 N ϵ distance was 28.4 Å compared to

16.5 Å in Figure 4A. In addition, weakened interior dipole moments favored the disruption of backbone H-bonds, such that the native structure was torn apart by the +9 charge of the protein ion (Figure 3E).

The 33+/22- model with $CSF = 1$ exhibited a salt bridge network at the protein surface (Figure 4C), consistent with zwitterionic simulations on other proteins.^{19, 21, 41} A similar network persisted down to $CSF = 0.1$, reflecting the fact that moieties with a +1 and -1 net charge were excluded from rescaling (Figure 4D). This salt bridge network prevented Coulombic expansion of hMb, such that even for $CSF = 0.1$ the 33+/22- model still produced collision cross sections that were close to the experimental Ω (Figure 2D).

In summary, charge rescaling can alter the balance between Coulombic repulsion and charge solvation in the gas phase. The use of atomic charges that are less polarized favors the loss of solution-like structure by suppressing electrostatic screening of protonated surface sites, and by weakening internal contacts such as backbone H-bonds. However, these disruptive effects only start to become significant under conditions that fall outside the physically reasonable range (such as $CSF = 0.1$ or 0.5). No major changes in protein behavior were discernible when comparing $CSF = 0.8$ runs with data obtained for the unmodified force field.^{68, 79-83} In other words, removing the water-linked overpolarization does not have major repercussions for the hMb gas phase simulations conducted here.

Collision-Induced Dissociation of TTR. As a next step we scrutinized the effects of charge rescaling by focusing on a more challenging problem. Transthyretin (TTR) is a homotetrameric protein that is commonly used as test system for native ESI. Collision-induced dissociation (CID) of TTR and most other complexes causes ejection of a highly charged monomer. This behavior has been attributed to gradual unfolding of a single subunit, with H^+ transfer onto the unravelling chain prior to its ejection.^{40, 95-97} This phenomenon is illustrated

by the experiments of Figure 5, where CID of the TTR 15+ tetramer generated 8+ monomers and 7+ trimers as the main products. Additional products were observed as well, *i.e.*, 9+/7+/6+ monomers with their complementary trimers (Figure 5A, B). IMS data acquired at different collision voltages confirmed that the TTR 15+ tetramer underwent partial unfolding prior to monomer ejection (Figure 5C).⁹⁵

Mobile-Proton MD Simulations. The CID behavior of TTR and other complexes reflects the high mobility of H⁺ in gaseous polypeptide ions.^{63, 98} Static-proton MD simulations (as used above for hMb) are not suitable for modeling such processes. Luckily, mobile-proton algorithms are available that can capture the CID behavior of multiprotein assemblies.^{72, 87}

Mobile-proton MD simulations⁸⁷ on TTR 15+ were initially conducted with unmodified OPLS-AA/L parameters⁶⁷ ($CSF = 1$). The protein temperature was gradually raised to mimic the effects of collisional activation.⁹⁵ Protons were continuously redistributed over all basic and acidic sites, subject to minimization of an energy term that considers electrostatic interactions among charged sites, as well as proton affinities.⁸⁷ Temperatures below ~450 K produced compact structures that resembled the X-ray starting coordinates (Figure 5D, top). The close proximity of acidic and basic sites in these conformers caused the mobile-proton algorithm to generate numerous salt bridges such as Lys-NH₃⁺ ··· OOC-Asp. These motifs are electrostatically favorable due to their negative q_1q_2/r contribution to the overall energy. The presence of such zwitterionic contacts is consistent with experiments.^{41, 48}

Progressive heating of TTR 15+ triggered breakdown of the native-like structure, with transient local unfolding (illustrated for $T = 475$ K and 500 K in Figure 5D). Ultimately, the “magenta” subunit unfolded while remaining attached to the complex. This process was accompanied by Coulombically driven H⁺ migration onto the unravelling chain. For the trajectory of Figure 5D this process culminated in ejection of an 8+ monomer, leaving behind

a 7+ trimer. This asymmetric charge-partitioning matches the dominant experimental CID pathway (Figure 5B). The MD data of Figure 5D are consistent with previous work, where the energetics and structural events associated with the CID process have been discussed in detail.⁸⁷

Figure 5C illustrates that the pre-dissociation MD structures of TTR 15+ between 300 K and ~500 K had Ω values that fell within the range of the experimental distributions. This agreement suggests that the MD-generated TTR 15+ structures are reasonable candidates for the experimental gas phase species. Figure 5 confirms⁸⁷ that the mobile-proton MD approach used here is suitable for modeling the CID behavior of multiprotein complexes. Experimental observables such as product ion charge states and collision cross sections were reproduced quite well by these $CSF = 1$ simulations.

CID Simulations with Charge Rescaling. Mobile-proton MD simulations on TTR 15+ were conducted for CSF values between 1.0 and 0.1. Figure 6A illustrates gas phase structures at a relatively low temperature of 352 K. The conformations for CSF 1.0 and 0.8 were similar, retaining most secondary and tertiary elements. For $CSF = 0.5$ helices and sheets started to dissolve. This trend continued for $CSF = 0.1$, where two of the subunits began to unravel (Figure 6A, top to bottom). This structural breakdown resembles the hMb data of Figure 3, reflecting the weakening of charge-dipole and dipole-dipole contacts with decreasing CSF .

The mobile-proton algorithm is sensitive to the distance r between acidic and basic sites.⁸⁷ For closely packed proteins with small r values the formation of salt bridges is energetically favored, as noted above. When r values increase as a result of gradual unfolding, zwitterionic contacts tend to transition to their charge-neutralized form, driven by the high proton affinity of carboxylates (*e.g.*, $\text{Lys-NH}_3^+ \text{ } ^-\text{OOC-Asp} \rightarrow \text{Lys-NH}_2 \text{ HOOC-Asp}$).^{63, 87} These considerations explain the loss of salt bridges in Figure 6A, from 13 negative

sites (red spheres) for the compact $CSF = 1$ structure down to 3 negative sites for the more unfolded $CSF = 0.1$ conformation.

Gradual heating of TTR 15+ culminated in ejection of a highly charged monomer for all mobile-proton runs, regardless of CSF value. In all cases, the ejected subunits had a net charge close to the experimental value of $\sim 8+$ (Figure 6B). It is remarkable that this outcome is so robust, and that monomer ejection is consistently favored over other dissociation channels, such as splitting into two dimers.

Major CSF -related differences were observed regarding the temperature and time required for the monomers to separate from the complex during heating (Figure 6C). For $CSF = 1$ separation took place at temperatures around 560 K, while $CSF = 0.8$ caused dissociation at ~ 480 K. The use of even lower CSF values further reduced the ejection temperature, down to ~ 400 K for $CSF = 0.1$. The enhanced susceptibility to thermal dissociation reflects the reduced stability of intra- and intermolecular contacts arising from electrostatic rescaling, as noted above. Consistent with Figure 6A, the number of salt bridges at the moment of monomer/trimer separation decreased with decreasing CSF (Figure 6D).

In summary, our mobile-proton CID simulations were surprisingly insensitive to charge rescaling. MD runs with $CSF = 0.8$ produced results close to those obtained with the unmodified force field, culminating in monomer charge states that agreed well with experiments. Differences for CSF values of 1.0 and 0.8 were limited to subtle features such as separation time/temperature and the number of salt bridges. None of these features can be reliably quantified in experiments, and thus it cannot be decided which CSF value, 1.0 or 0.8, is more suitable for capturing the protein behavior in the vacuum of the mass spectrometer. As before, MD data with $CSF = 0.5$ and 0.1 were included here only for illustrative purposes, keeping in mind that they fall outside the physically reasonable range.^{68, 79-83}

Conclusions

The goal of this work was to scrutinize the performance of solution force fields for simulations on gaseous protein ions. An investigation of this type seemed warranted, considering how many MS studies have used CHARMM, OPLS-AA/L, etc. without considering possible pitfalls of the solution/gas phase mismatch. As a case in point, the widespread use of OPLS-AA/L for gas phase MD simulations is at odds with the fact that “OPLS” stands for “optimized potentials for liquid simulations”.⁶⁷

To account for an aqueous environment, the atomic charges of standard force fields are enhanced using empirical fitting methods, thereby generating an overpolarization of ~20% relative to vacuum *ab initio* calculations.^{67, 68, 79-83} Here we pursued a simple strategy to examine the implications of this overpolarization for the gas phase. Our approach employed a factor that uniformly reduced atomic charges, while preserving the net protein charge. Modifying the force field with $CSF = 0.8$ should roughly compensate for the ~20% overpolarization.^{67, 68, 79-83}

We found that gas phase protein data generated with $CSF = 0.8$ were very close to those obtained with unmodified parameters. In other words, the simulation outcomes are quite insensitive to moderate alterations of atomic charges. Systematic errors associated with the use of solution force fields for gas phase protein simulations, therefore, appear to be relatively small. Dedicated vacuum force fields are not currently available. For the time being, it thus seems acceptable to continue the use of solution force fields (such as CHARMM and OPLS-AA/L) for gaseous protein ions. These solution force fields are unlikely to produce highly accurate gas phase results, but they provide semi-quantitative information that will be sufficient for addressing basic questions related to protein structure and dynamics *in vacuo*. These include the mechanism(s) by which solution-like conformers

undergo kinetic trapping,⁸⁻¹² the collapse of internal cavities,²²⁻²⁴ and the orientational preferences of surface side chains.¹⁹⁻²¹

Several reasons can be identified for the apparent robustness of solution force fields in the gas phase. (1) Despite being optimized for an aqueous environment, standard force fields are designed to maintain basic gas phase functionality, as verified by structural and energetic benchmarking against *ab initio* data. This is particularly true for the OPLS-AA/L force field.^{67, 99} (2) Compact globular protein ions produced by native ESI have most of their atoms buried in the interior. The environment of these atoms will not undergo major changes during protein transfer into the gas phase. Solution force fields should provide a reasonable description of these buried moieties, and parameters derived for a genuine gas phase environment would likely be less appropriate.⁷⁸ (3) The current lack of high resolution structure determination methods in the gas phase undoubtedly masks some of the imperfections associated with the application of standard MD force fields to electrosprayed protein ions.

The findings of the current work will be welcome news for the many practitioners who have applied solution force fields to gaseous protein ions in the past. Despite the remarkable robustness of standard parameter sets such as CHARMM and OPLS-AA/L for gas phase applications, it is hoped that future developments will yield *bona fide* gas phase MD strategies. Features that should be explicitly addressed include dynamic polarization effects, the possible rupture and formation of covalent bonds, as well as mobile-proton strategies that go beyond the simple approach used here. Many of these tools already exist, but the challenge is to implement them in a way that allows large biomolecular systems to be studied on time scales of milliseconds and beyond. Coarse-grained models could help address time scale limitations,¹⁰⁰ but the loss of molecular details inherent to such approaches might not be acceptable for all applications.

Acknowledgments. Funding for this work was provided by the Natural Sciences and Engineering Research Council of Canada (RGPIN-2018-04243). We thank Dr. Haidy Metwally for acquiring the experimental data of Figure 2.

References

- (1) Fenn, J. B. Electrospray wings for molecular elephants (nobel lecture). *Angew. Chem. Int. Ed.* **2003**, *42*, 3871-3894.
- (2) Leney, A. C.; Heck, A. J. R. Native mass spectrometry: What is in the name? *J. Am. Soc. Mass Spectrom.* **2017**, *28*, 5-13.
- (3) Nguyen, G. T. H.; Tran, T. N.; Podgorski, M. N.; Bell, S. G.; Supuran, C. T.; Donald, W. A. Nanoscale ion emitters in native mass spectrometry for measuring ligand–protein binding affinities. *ACS Centr. Sci.* **2019**, *5*, 308–318.
- (4) Peetz, O.; Hellwig, N.; Henrich, E.; Mezhyrova, J.; Dotsch, V.; Bernhard, F.; Morgner, N. Lilbid and nesi: Different native mass spectrometry techniques as tools in structural biology. *J. Am. Soc. Mass Spectrom.* **2019**, *30*, 181-191.
- (5) Fatunmbi, O.; Abzalimov, R. R.; Savinov, S. N.; Gershenson, A.; Kaltashov, I. A. Interactions of haptoglobin with monomeric globin species: Insights from molecular modeling and native electrospray ionization mass spectrometry. *Biochemistry* **2016**, *55*, 1918-1928.
- (6) Bush, M. F.; Hall, Z.; Giles, K.; Hoyes, J.; Robinson, C. V.; Ruotolo, B. T. Collision cross sections of proteins and their complexes: A calibration framework and database for gas-phase structural biology. *Anal. Chem.* **2010**, *82*, 9667-9565.
- (7) Jurneczko, E.; Barran, P. E. How useful is ion mobility mass spectrometry for structural biology? The relationship between protein crystal structures and their collision cross sections in the gas phase. *Analyst* **2011**, *136*, 20-28.
- (8) Meyer, T.; Gabelica, V.; Grubmueller, H.; Orozco, M. Proteins in the gas phase. *WIREs Comput. Mol. Sci.* **2013**, *3*, 408-425.
- (9) Hamdy, O. M.; Julian, R. R. Reflections on charge state distributions, protein structure, and the mystical mechanism of electrospray ionization. *J. Am. Soc. Mass Spectrom.* **2012**, *23*, 1-6.
- (10) Clemmer, D. E.; Russell, D. H.; Williams, E. R. Characterizing the conformationome: Toward a structural understanding of the proteome. *Accounts Chem. Res.* **2017**, *50*, 556-560.
- (11) Bleiholder, C.; Liu, F. C. Structure relaxation approximation (sra) for elucidation of protein structures from ion mobility measurements. *J. Phys. Chem. B* **2019**, *123*, 2756-2769.
- (12) Wolynes, P. G. Biomolecular folding in vacuo!!!(?). *Proc. Natl. Acad. Sci. U.S.A.* **1995**, *92*, 2426-2427.
- (13) Porrini, M.; Rosu, F.; Rabin, C.; Darre, L.; Gomez, H.; Orozco, M.; Gabelica, V. Compaction of duplex nucleic acids upon native electrospray mass spectrometry. *ACS Central Sci.* **2017**, *3*, 454–461.
- (14) Czar, M. F.; Zosel, F.; Koenig, I.; Nettels, D.; Wunderlich, B.; Schuler, B.; Zarrine-Afsar, A.; Jockusch, R. A. Gas-phase fret efficiency measurements to probe the conformation of mass-selected proteins. *Anal. Chem.* **2015**, *87*, 7559-7565.
- (15) Devine, P. W. A.; Fisher, H. C.; Calabrese, A. N.; Whelan, F.; Higazi, D. R.; Potts, J. R.; Lowe, D. C.; Radford, S. E.; Ashcroft, A. E. Investigating the structural compaction of biomolecules upon transition to the gas-phase using esi-twins-ms. *J. Am. Soc. Mass Spectrom.* **2017**, *28*, 1855-1862.
- (16) Ly, T.; Julian, R. R. Elucidating the tertiary structure of protein ions in vacuo with site specific photoinitiated radical reactions. *J. Am. Chem. Soc.* **2010**, *132*, 8602-8609.
- (17) Skinner, O. S.; McLafferty, F. W.; Breuker, K. How ubiquitin unfolds after transfer into the gas phase. *J. Am. Soc. Mass Spectrom.* **2012**, *23*, 1011-1014.

- (18) Hansen, K.; Lau, A. M.; Giles, K.; McDonnell, J. M.; Struwe, W. B.; Sutton, B. J.; Politis, A. A mass-spectrometry-based modelling workflow for accurate prediction of igg antibody conformations in the gas phase. *Angew. Chem.-Int. Edit.* **2018**, *57*, 17194-17199.
- (19) Bakhtiari, M.; Konermann, L. Protein ions generated by native electrospray ionization: Comparison of gas phase, solution, and crystal structures. *J. Phys. Chem. B* **2019**, *123*, 1784-1796.
- (20) Shelimov, K. B.; Clemmer, D. E.; Hudgins, R. R.; Jarrold, M. F. Protein structure in vacuo: The gas-phase conformation of bpti and cytochrome c. *J. Am. Chem. Soc.* **1997**, *119*, 2240-2248.
- (21) Steinberg, M. Z.; Elber, R.; McLafferty, F. W.; Gerber, R. B.; Breuker, K. Early structural evolution of native cytochrome c after solvent removal. *ChemBioChem* **2008**, *9*, 2417-2423.
- (22) Hall, Z.; Politis, A.; Bush, M. F.; Smith, L. J.; Robinson, C. V. Charge-state dependent compaction and dissociation of protein complexes: Insights from ion mobility and molecular dynamics. *J. Am. Chem. Soc.* **2012**, *134*, 3429-3438.
- (23) Hogan, C. J.; Ruotolo, B. T.; Robinson, C. V.; de la Mora, J. F. Tandem differential mobility analysis-mass spectrometry reveals partial gas-phase collapse of the groel complex. *J. Phys. Chem. B* **2011**, *115*, 3614-3621.
- (24) Michaelevski, I.; Eisenstein, M.; Sharon, M. Gas-phase compaction and unfolding of protein structures. *Anal. Chem.* **2010**, *82*, 9484-9491.
- (25) Barylyuk, K.; Balabin, R. M.; Grunstein, D.; Kikkeri, R.; Frankevich, V.; Seeberger, P. H.; Zenobi, R. What happens to hydrophobic interactions during transfer from the solution to the gas phase? The case of electrospray-based soft ionization methods. *J. Am. Soc. Mass Spectrom.* **2011**, *22*, 1167-1177.
- (26) Liu, L.; Bagal, D.; Kitova, E. N.; Schnier, P. D.; Klassen, J. S. Hydrophobic protein-ligand interactions preserved in the gas phase. *J. Am. Chem. Soc.* **2009**, *131*, 15980-15981.
- (27) Beveridge, R.; Phillips, A. S.; Denbigh, L.; Saleem, H. M.; MacPhee, C. E.; Barran, P. E. Relating gas phase to solution conformations: Lessons from disordered proteins. *Proteomics* **2015**, *15*, 2872-2883.
- (28) Chen, S.-H.; Russell, D. H. How closely related are conformations of protein ions sampled by im-ms to native solution structures? *J. Am. Soc. Mass Spectrom.* **2015**, *26*, 1433-1443.
- (29) Bogan, M. J. X-ray free electron lasers motivate bioanalytical characterization of protein nanocrystals: Serial femtosecond crystallography. *Anal. Chem.* **2013**, *85*, 3464-3471.
- (30) Rosenbaum, D. M.; Cherezov, V.; Hanson, M. A.; Rasmussen, S. G. F.; Thian, F. S.; Kobilka, T. S.; Choi, H.; Yao, X.; Weis, W. I.; Stevens, R. C., et al. GPCR engineering yields high-resolution structural insights into β 2-adrenergic receptor function. *Science* **2007**, *318*, 1266-1273.
- (31) Dubochet, J. On the development of electron cryo-microscopy (nobel lecture). *Angew. Chem.-Int. Edit.* **2018**, *57*, 10842-10846.
- (32) Wuthrich, K. Nmr studies of structure and function of biological macromolecules (nobel lecture). *Angew. Chem.-Int. Edit.* **2003**, *42*, 3340-3363.
- (33) Wyttenbach, T.; Pierson, N. A.; Clemmer, D. E.; Bowers, M. T. Ion mobility analysis of molecular dynamics. *Annu. Rev. Phys. Chem.* **2014**, *65*, 175-196.
- (34) Gabelica, V.; Marklund, E. Fundamentals of ion mobility spectrometry. *Curr. Op. Chem. Biol.* **2017**, *42*, 51-59.
- (35) Silveira, J. A.; Servage, K. A.; Gamage, C. M.; Russell, D. H. Cryogenic ion mobility-mass spectrometry captures hydrated ions produced during electrospray ionization. *J. Phys. Chem. A* **2013**, *117*, 953-961.

- (36) Lee, J. W.; Davidson, K. L.; Bush, M. F.; Kim, H. I. Collision cross sections and ion structures: Development of a general calculation method via high-quality ion mobility measurements and theoretical modeling. *Analyst* **2017**, *142*, 4289-4298.
- (37) Campuzano, I. D. G.; Lippens, J. L. Ion mobility in the pharmaceutical industry: An established biophysical technique or still niche? *Curr. Op. Chem. Biol.* **2018**, *42*, 147-159.
- (38) Pepin, R.; Laszlo, K. J.; Marek, A.; Peng, B.; Bush, M. F.; Lavanant, H.; Afonso, C.; Turecek, F. Toward a rational design of highly folded peptide cation conformations. 3d gas-phase ion structures and ion mobility characterization. *J. Am. Soc. Mass Spectrom.* **2016**, *27*, 1647-1660.
- (39) Politis, A.; Park, A. Y.; Hyung, S.-J.; Barsky, D.; Ruotolo, B. T.; Robinson, C. V. Integrating ion mobility mass spectrometry with molecular modelling to determine the architecture of multiprotein complexes. *PLoS ONE* **2010**, *5*, e12080.
- (40) Quintyn, R. S.; Zhou, M.; Yan, J.; Wysocki, V. H. Surface-induced dissociation mass spectra as a tool for distinguishing different structural forms of gas-phase multimeric protein complexes. *Anal. Chem.* **2015**, *87*, 11879-11886.
- (41) Bonner, J. G.; Lyon, Y. A.; Nellessen, C.; Julian, R. R. Photoelectron transfer dissociation reveals surprising favorability of zwitterionic states in large gaseous peptides and proteins. *J. Am. Chem. Soc.* **2017**, *139*, 10286-10293.
- (42) Morrison, L. J.; Brodbelt, J. S. 193 nm ultraviolet photodissociation mass spectrometry of tetrameric protein complexes provides insight into quaternary and secondary protein topology. *J. Am. Chem. Soc.* **2016**, *138*, 10849-10859.
- (43) Li, H. L.; Nguyen, H. H.; Ogorzalek Loo, R. R.; Campuzano, I. D. G.; Loo, J. A. An integrated native mass spectrometry and top-down proteomics method that connects sequence to structure and function of macromolecular complexes. *Nat. Chem.* **2018**, *10*, 139-148.
- (44) Lermyte, F.; Konijnenberg, A.; Williams, J. P.; Brown, J. M.; Valkenburg, D.; Sobott, F. Etd allows for native surface mapping of a 150 kDa noncovalent complex on a commercial q-twims-tof instrument. *J. Am. Soc. Mass Spectrom.* **2014**, *25*, 343-350.
- (45) Zhang, H.; Cui, W.; Gross, M. L. Native electrospray ionization and electron-capture dissociation for comparison of protein structure in solution and the gas phase. *Int. J. Mass Spectrom.* **2013**, *354-355*, 288-291.
- (46) Benesch, J. L. P. Collisional activation of protein complexes: Picking up the pieces. *J. Am. Soc. Mass Spectrom.* **2009**, *20*, 341-348.
- (47) Horn, D. M.; Breuker, K.; Frank, A. J.; McLafferty, F. W. Kinetic intermediates in the folding of gaseous protein ions characterized by electron capture dissociation mass spectrometry. *J. Am. Chem. Soc.* **2001**, *123*, 9792-9799.
- (48) Seo, J.; Warnke, S.; Pagel, K.; Bowers, M. T.; von Helden, G. Infrared spectrum and structure of the homochiral serine octamer-dichloride complex. *Nat. Chem.* **2017**, *9*, 1263-1268.
- (49) Frankevich, V.; Barylyuk, K.; Chingin, K.; Nieckarz, R.; Zenobi, R. Native biomolecules in the gas phase? The case of green fluorescent protein. *ChemPhysChem.* **2013**, *14*, 929-935.
- (50) Mistarz, U. H.; Brown, J. M.; Haselmann, K. F.; Rand, K. D. Probing the binding interfaces of protein complexes using gas-phase h/d exchange mass spectrometry. *Structure* **2016**, *24*, 310-318.
- (51) Karanji, A. K.; Khakinejad, M.; Kondalaji, S. G.; Majuta, S. N.; Attanayake, K.; Valentine, J. S. Comparison of peptide ion conformers arising from non-helical and helical peptides using ion mobility spectrometry and gas-phase hydrogen/deuterium exchange. *J. Am. Soc. Mass Spectrom.* **2018**, *29*, 2402-2412.
- (52) Becke, A. D. Perspective: Fifty years of density-functional theory in chemical physics. *J. Chem. Phys.* **2014**, *140*, 18A3011-18A30118.

- (53) Chen, Y.; Rodgers, M. T. Structural and energetic effects in the molecular recognition of amino acids by 18-crown-6. *J. Am. Chem. Soc.* **2012**, *134*, 5863-5875.
- (54) Bell, M. R.; Cruzeiro, V. W. D.; Cismesia, A. P.; Tesler, L. F.; Roitberg, A. E.; Polfer, N. C. Probing the structures of solvent-complexed ions formed in electrospray ionization using cryogenic infrared photodissociation spectroscopy. *J. Phys. Chem. A* **2018**, *122*, 7427-7436.
- (55) Jockusch, R. A.; Price, W. D.; Williams, E. R. Structure of cationized arginine (arg center dot m⁺, m = h, li, na, k, rb, and cs) in the gas phase: Further evidence for zwitterionic arginine. *J. Phys. Chem. A* **1999**, *103*, 9266-9274.
- (56) Turecek, F. Benchmarking electronic excitation energies and transitions in peptide radicals. *J. Phys. Chem. A* **2015**, *119*, 10101-10111.
- (57) Chen, M.; Zheng, L. X.; Santra, B.; Ko, H. Y.; DiStasio, R. A.; Klein, M. L.; Car, R.; Wu, X. F. Hydroxide diffuses slower than hydronium in water because its solvated structure inhibits correlated proton transfer. *Nat. Chem.* **2018**, *10*, 413-419.
- (58) Hassanali, A.; Giberti, F.; Cuny, J.; Kuhne, T. D.; Parrinello, M. Proton transfer through the water gossamer. *Proc. Natl. Acad. Sci. U. S. A.* **2013**, *110*, 13723-13728.
- (59) Zhao, T. S.; Zhou, J.; Wang, Q.; Jena, P. Like charges attract? *J. Phys. Chem. Lett.* **2016**, *7*, 2689-2695.
- (60) Pepin, R.; Petrone, A.; Laszlo, K. J.; Bush, M. F.; Li, X. S.; Turecek, F. Does thermal breathing affect collision cross sections of gas-phase peptide ions? An ab initio molecular dynamics study. *J. Phys. Chem. Lett.* **2016**, *7*, 2765-2771.
- (61) Scutelnic, V.; Perez, M. A. S.; Marianski, M.; Warnke, S.; Gregor, A.; Rothlisberger, U.; Bowers, M. T.; Baldauf, C.; von Helden, G.; Rizzo, T. R., et al. The structure of the protonated serine octamer. *J. Am. Chem. Soc.* **2018**, *140*, 7554-7560.
- (62) Arcella, A.; Dreyer, J.; Ippoliti, E.; Ivani, I.; Portella, G.; Gabelica, V.; Carloni, P.; Orozco, M. Structure and dynamics of oligonucleotides in the gas phase. *Angew. Chem.-Int. Edit.* **2015**, *54*, 467-471.
- (63) Li, J. Y.; Lyu, W. P.; Rossetti, G.; Konijnenberg, A.; Natalello, A.; Ippoliti, E.; Orozco, M.; Sobott, F.; Grandori, R.; Carloni, P. Proton dynamics in protein mass spectrometry. *J. Phys. Chem. Lett.* **2017**, *8*, 1105-1112.
- (64) Barnes, G. L.; Podczewinski, A. Simulating the effect of charge state on reactive landing of a cyclic tetrapeptide on chemically modified alkythiolate self-assembled monolayer surfaces. *J. Phys. Chem. C* **2017**, *121*, 14628-14635.
- (65) Cleary, S. P.; Prell, J. S. Liberating native mass spectrometry from dependence on volatile salt buffers by use of gabor transform. *Chemphyschem* **2019**, *20*, 519-523.
- (66) Gulbakan, B.; Barylyuk, K.; Schneider, P.; Pillong, M.; Schneider, G.; Zenobi, R. Native electrospray ionization mass spectrometry reveals multiple facets of aptamer-ligand interactions: From mechanism to binding constants. *J. Am. Chem. Soc.* **2018**, *140*, 7486-7497.
- (67) Kaminski, G. A.; Friesner, R. A.; Tirado-Rives, J.; Jorgensen, W. L. Evaluation and reparametrization of the opl-aa force field for proteins via comparison with accurate quantum chemical calculations on peptides. *J. Phys. Chem. B* **2001**, *105*, 6474-6487.
- (68) Hornak, V.; Abel, R.; Okur, A.; Strockbine, B.; Roitberg, A.; Simmerling, C. Comparison of multiple amber force fields and development of improved protein backbone parameters. *Proteins* **2006**, *65*, 712-725.
- (69) Huang, J.; MacKerell, A. D. Charmm36 all-atom additive protein force field: Validation based on comparison to nmr data. *J. Comput. Chem.* **2013**, *34*, 2135-2145.
- (70) Abraham, M. J.; Murtola, T.; Schulz, R.; Páll, S.; Smith, J. C.; Hess, B.; Lindahl, E. Gromacs: High performance molecular simulations through multi-level parallelism from laptops to supercomputers. *SoftwareX* **2015**, *1-2*, 19-25.

- (71) Patriksson, A.; Adams, C. M.; Kjeldsen, F.; Zubarev, R. A.; van der Spoel, D. A direct comparison of protein structure in the gas and solution phase: The trp-cage. *J. Phys. Chem. B* **2007**, *111*, 13147-13150.
- (72) Fegan, S. K.; Thachuk, M. A charge moving algorithm for molecular dynamics simulations of gas-phase proteins. *J. Chem. Theory Comput.* **2013**, *9*, 2531-2539.
- (73) Mao, Y.; Ratner, M. A.; Jarrold, M. F. Molecular dynamics simulations of the charge-induced unfolding and refolding of unsolvated cytochrome c. *J. Phys. Chem. B* **1999**, *103*, 10017-10021.
- (74) Albrieux, F.; Calvo, F.; Chirot, F.; Vorobyev, A.; Tsybin, Y. O.; Lepère, V.; Antoine, R.; Lemoine, J.; Dugourd, P. Conformation of polyalanine and polyglycine dications in the gas phase: Insight from ion mobility spectrometry and replica-exchange molecular dynamics. *J. Phys. Chem. A* **2010**, *114*, 6888-6896.
- (75) Schenk, E. R.; Almeida, R.; Miksovska, J.; Ridgeway, M. E.; Park, M. A.; Fernandez-Lima, F. Kinetic intermediates of holo- and apo-myoglobin studied using hdx-tims-ms and molecular dynamic simulations. *J. Am. Soc. Mass Spectrom.* **2015**, *26*, 555-563.
- (76) Kulesza, A.; Marklund, E. G.; MacAleese, L.; Chirot, F.; Dugourd, P. Bringing molecular dynamics and ion-mobility spectrometry closer together: Shape correlations, structure-based predictors, and dissociation. *J. Phys. Chem. B* **2018**, *122*, 8317-8329.
- (77) Jorgensen, W. L.; Maxwell, D. S.; TiradoRives, J. Development and testing of the opls all-atom force field on conformational energetics and properties of organic liquids. *J. Am. Chem. Soc.* **1996**, *118*, 11225-11236.
- (78) Konermann, L.; Metwally, H.; McAllister, R. G.; Popa, V. How to run molecular dynamics simulations on electrospray droplets and gas phase proteins: Basic guidelines and selected applications. *Methods* **2018**, *144*, 104-112.
- (79) Mackerell, A. D. Empirical force fields for biological macromolecules: Overview and issues. *J. Comput. Chem.* **2004**, *25*, 1584-1604.
- (80) Lemkul, J. A.; Huang, J.; Roux, B.; MacKerell, A. D. An empirical polarizable force field based on the classical drude oscillator model: Development history and recent applications. *Chem. Rev.* **2016**, *116*, 4983-5013.
- (81) Liu, H. C.; Wang, Y. M.; Bowman, J. M. Transferable ab initio dipole moment for water: Three applications to bulk water. *J. Phys. Chem. B* **2016**, *120*, 1735-1742.
- (82) Abascal, J. L. F.; Vega, C. A general purpose model for the condensed phases of water: Tip4p/2005. *J. Chem. Phys.* **2005**, *123*, 234505.
- (83) Ponder, J. W.; Case, D. A., Force fields for protein simulations. In *Advances in protein chemistry*, Elsevier: Amsterdam, 2003; Vol. 66, pp 27-84.
- (84) Kaminski, G. A.; Stern, H. A.; Berne, B. J.; Friesner, R. A.; Cao, Y. X. X.; Murphy, R. B.; Zhou, R. H.; Halgren, T. A. Development of a polarizable force field for proteins via ab initio quantum chemistry: First generation model and gas phase tests. *J. Comput. Chem.* **2002**, *23*, 1515-1531.
- (85) Kaltashov, I. A.; Fenselau, C. Stability of secondary structural elements in a solvent-free environment: The alpha helix. *Proteins* **1997**, *27*, 165-170.
- (86) Sun, Y.; Vahidi, S.; Sowole, M. A.; Konermann, L. Protein structural studies by traveling wave ion mobility spectrometry: A critical look at electrospray sources and calibration issues. *J. Am. Soc. Mass Spectrom.* **2016**, *27*, 31-40.
- (87) Popa, V.; Trecroce, D. A.; McAllister, R. G.; Konermann, L. Collision-induced dissociation of electrosprayed protein complexes: An all-atom molecular dynamics model with mobile protons. *J. Phys. Chem. B* **2016**, *120*, 5114-5124.
- (88) Ewing, S. A.; Donor, M. T.; Wilson, J. W.; Prell, J. S. Collidoscope: An improved tool for computing collisional cross-sections with the trajectory method. *J. Am. Soc. Mass Spectrom.* **2017**, *28*, 587-596.

- (89) Dobo, A.; Kaltashov, I. A. Detection of multiple protein conformational ensembles in solution via deconvolution of charge-state distributions in esi ms. *Anal. Chem.* **2001**, *73*, 4763-4773.
- (90) Hopper, J. T. S.; Oldham, N. J. Collision induced unfolding of protein ions in the gas phase studied by ion mobility-mass spectrometry: The effect of ligand binding on conformational stability. *J. Am. Soc. Mass Spectrom.* **2009**, *20*, 1851-1858.
- (91) Ogorzalek Loo, R. R.; Loo, J. A. Salt bridge rearrangement (sabre) explains the dissociation behavior of noncovalent complexes. *J. Am. Soc. Mass Spectrom.* **2016**, *27*, 975-990.
- (92) Schnier, P. D.; Gross, D. S.; Williams, E. R. Electrostatic forces and dielectric polarizability of multiply protonated gas-phase cytochrome c ions probed by ion/molecule chemistry. *J. Am. Chem. Soc.* **1995**, *117*, 6747-6757.
- (93) Warnke, S.; von Helden, G.; Pagel, K. Protein structure in the gas phase: The influence of side-chain microsolvation. *J. Am. Chem. Soc.* **2013**, *135*, 1177-1180.
- (94) Marchese, R.; Grandori, R.; Carloni, P.; Raugei, S. On the zwitterionic nature of gas-phase peptides and protein ions. *PLoS Comput. Biol.* **2010**, *6*, e1000775.
- (95) Ruotolo, B. T.; Hyung, S.-J.; Robinson, P. M.; Giles, K.; Bateman, R. H.; Robinson, C. V. Ion mobility-mass spectrometry reveals long-lived, unfolded intermediates in the dissociation of protein complexes. *Angew. Chem. Int. Ed.* **2007**, *46*, 8001-8004.
- (96) Felitsyn, N.; Kitova, E. N.; Klassen, J. S. Thermal decomposition of a gaseous multiprotein complex studied by blackbody infrared radiative dissociation. Investigating the origin of the asymmetric dissociation behavior. *Anal. Chem.* **2001**, *73*, 4647-4661.
- (97) Abzalimov, R. R.; Frimpong, A. K.; Kaltashov, I. A. Gas-phase processes and measurements of macromolecular properties in solution: On the possibility of false positive and false negative signals of protein unfolding. *Int. J. Mass Spectrom.* **2006**, *253*, 207-216.
- (98) Dongré, A. R.; Jones, J. L.; Somogyi, Á.; Wysocki, V. H. Influence of peptide composition, gas-phase basicity, and chemical modification on fragmentation efficiency: Evidence for the mobile proton model. *J. Am. Chem. Soc.* **1996**, *118*, 8365-8374.
- (99) Beachy, M. D.; Chasman, D.; Murphy, R. B.; Halgren, T. A.; Friesner, R. A. Accurate ab initio quantum chemical determination of the relative energetics of peptide conformations and assessment of empirical force fields. *J. Am. Chem. Soc.* **1997**, *119*, 5908-5920.
- (100) Marrink, S. J.; Tieleman, D. P. Perspective on the martini model. *Chem. Soc. Rev.* **2013**, *42*, 6801-6822.

Figure Captions

Figure 1. Arbitrary hexapeptide, with partial atomic charges as defined in the OPLS-AA/L force field.⁶⁷ The four titratable sites are in their charged forms, i.e., positive for N-terminus (NT), positive for the Lys side chain, negative for the Asp side chain, and negative for the C-terminus (CT). Coloring of elements: Carbon, green; nitrogen, blue; oxygen, red; hydrogen, light gray.

Figure 2. (A) Native ESI mass spectrum of hMb. (B) IMS characterization of hMb 9+. (C) Calculated collision cross section Ω of hMb 9+ after 1 μ s gas phase MD simulations, using a 11+/2- protonation pattern. Bars represent Ω values for different charge scaling factors (*CSF*). (D) Same as panel C, but for a 31+/22- protonation pattern. The red dashed lines in panels C/D indicate the experimental Ω value from panel B.

Figure 3. (A) Crystal structure of hMb (1wla). Heme is shown in red; the eight helices “A” to “H” are colored individually. All other panels show 1 μ s MD structures of gaseous hMb 9+ for different charge scaling factors (*CSF*). (B-E) 11+/2- protonation pattern. (F-I) 31+/22- protonation pattern. Positively and negatively charged residues are marked in cyan and red, respectively. Side chains have been omitted to reduce clutter. RMSD values relative to the initial crystal structures for B-E (in nm): 0.28, 0.31, 0.56, 1.24. For F-I: 0.29, 0.39, 0.66, 0.67.

Figure 4. Close-ups of 1 μ s MD structures for hMb 9+ in the gas phase. (A, B) 11+/2- pattern. (C, D) 31+/22- pattern. Positively and negatively charged residues are marked with

cyan and red spheres, respectively. Several neutral residues are highlighted using black labels. Not all side chains are shown to reduce clutter.

Figure 5. ESI mass spectra of tetrameric TTR 15+ after precursor ion selection (A) under gentle conditions, and (B) after CID, giving rise to monomeric “M” and trimeric “T” products. (C) Colored lines represent experimental IMS profiles of the 15+ tetramer at different collision voltages. (D) Mobile-proton MD simulation of TTR 15+ with gradual heating, using $CSF = 1$. Subunits are shown in different colors. The net charge of the “magenta” subunit is indicated; it eventually leaves as a 8+ ion. Also shown are the temperature and simulation time for each MD snapshot. Vertical lines in panel C represent Ω values of TTR 15+ MD structures at different temperature (standard deviations are $\sim 2.5\%$).

Figure 6. Mobile-proton MD results for the CID process of the TTR 15+ tetramer, for different CSF values. (A) TTR structures close to the onset of collisional heating. Positively and negatively charged residues are marked cyan and red, respectively. (B) Net charge of the ejected monomer. (C) Time and temperature where the monomer separates from the complex. (D) Total number of salt bridges in the tetramer at the separation point.

Figure 2

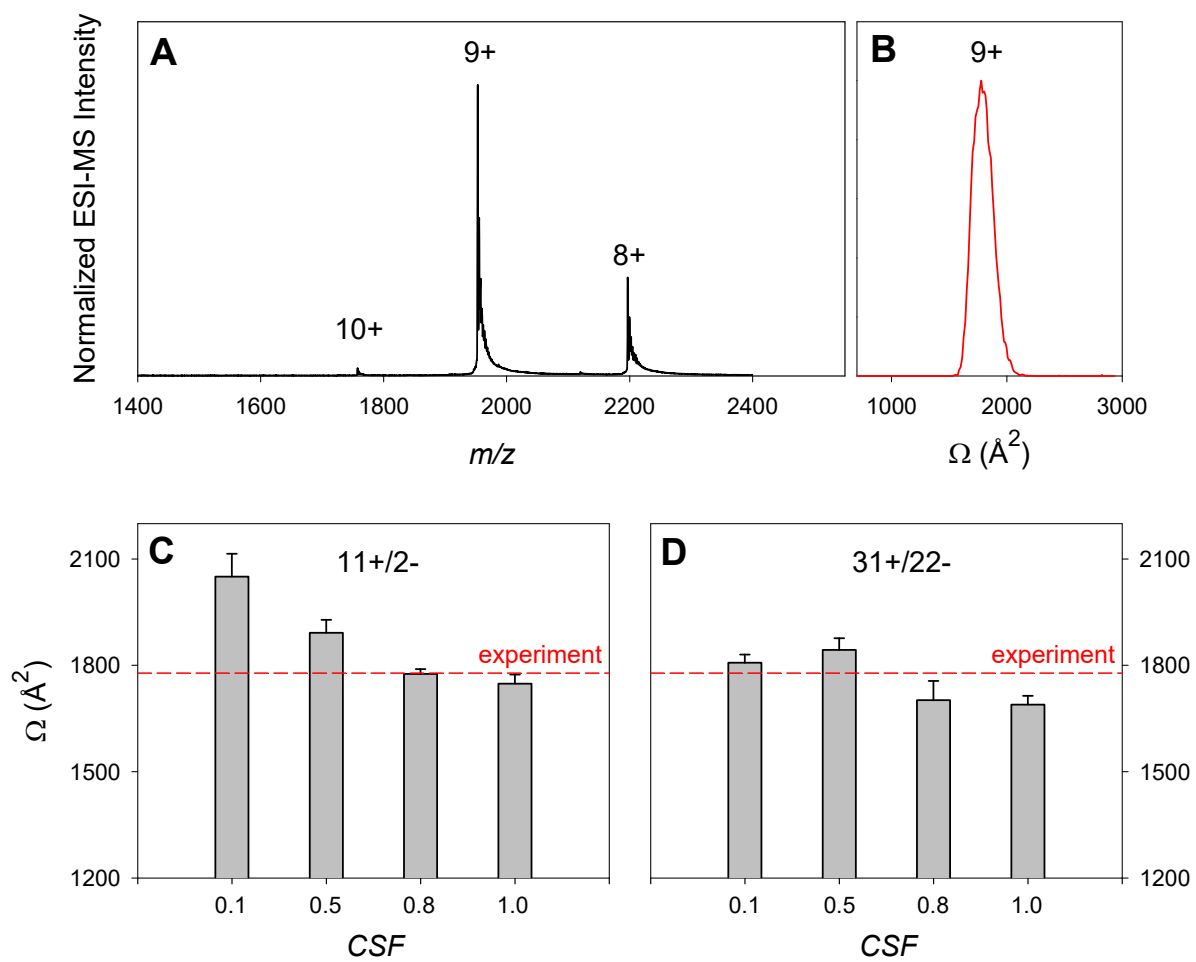


Figure 3

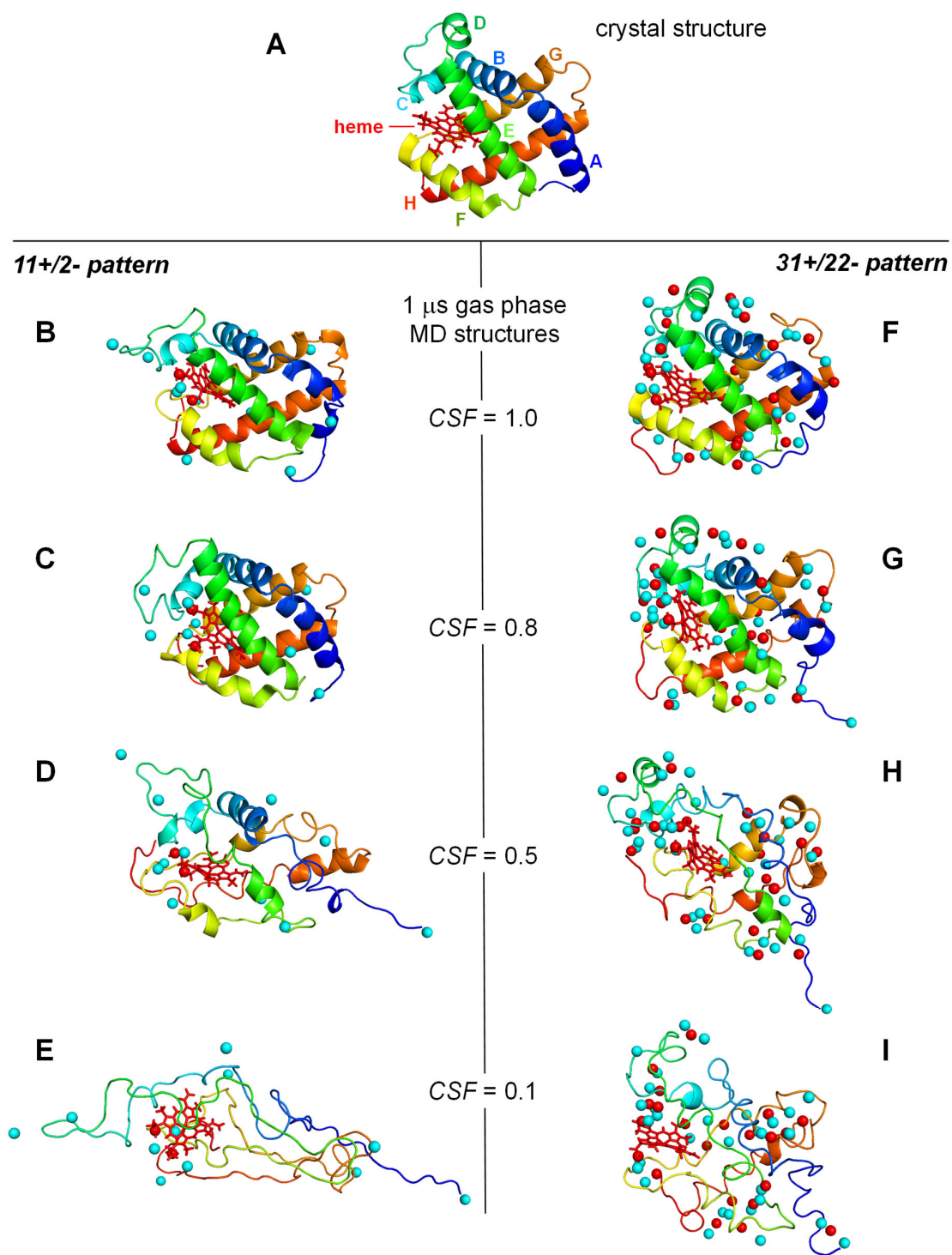


Figure 4

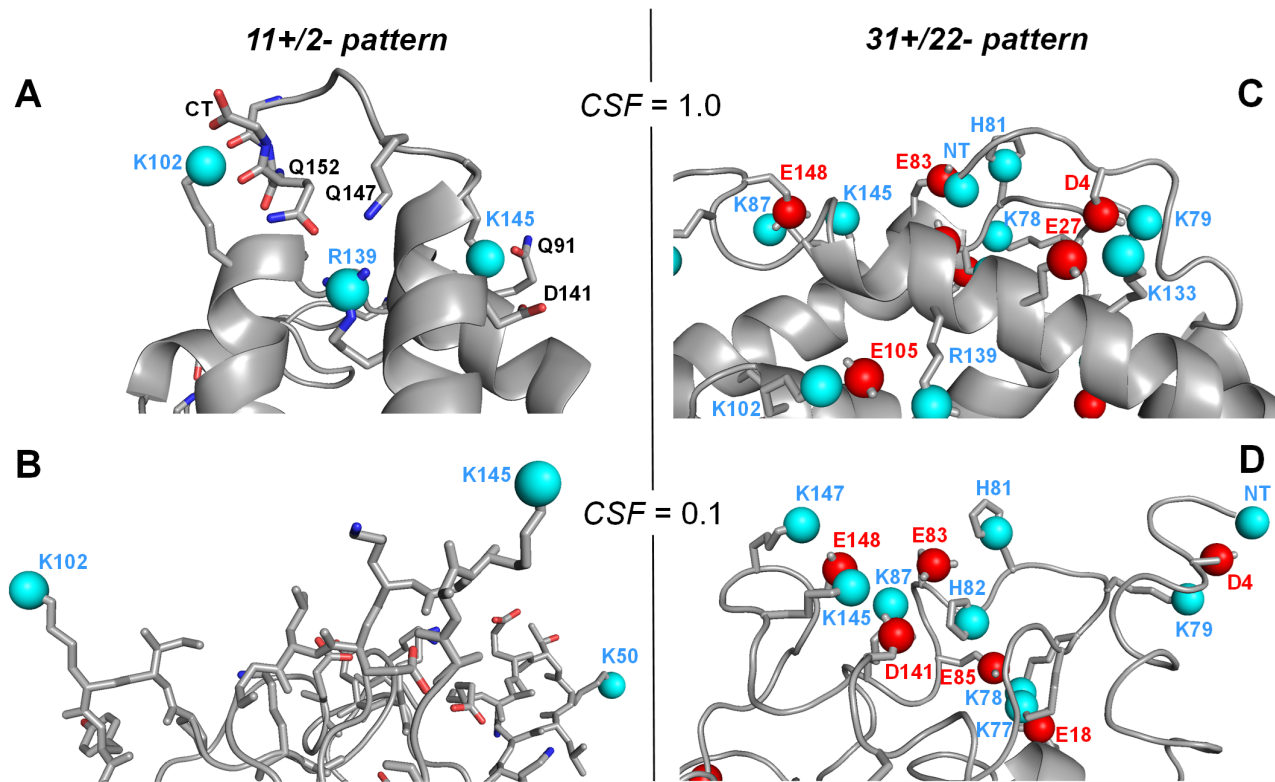


Figure 5

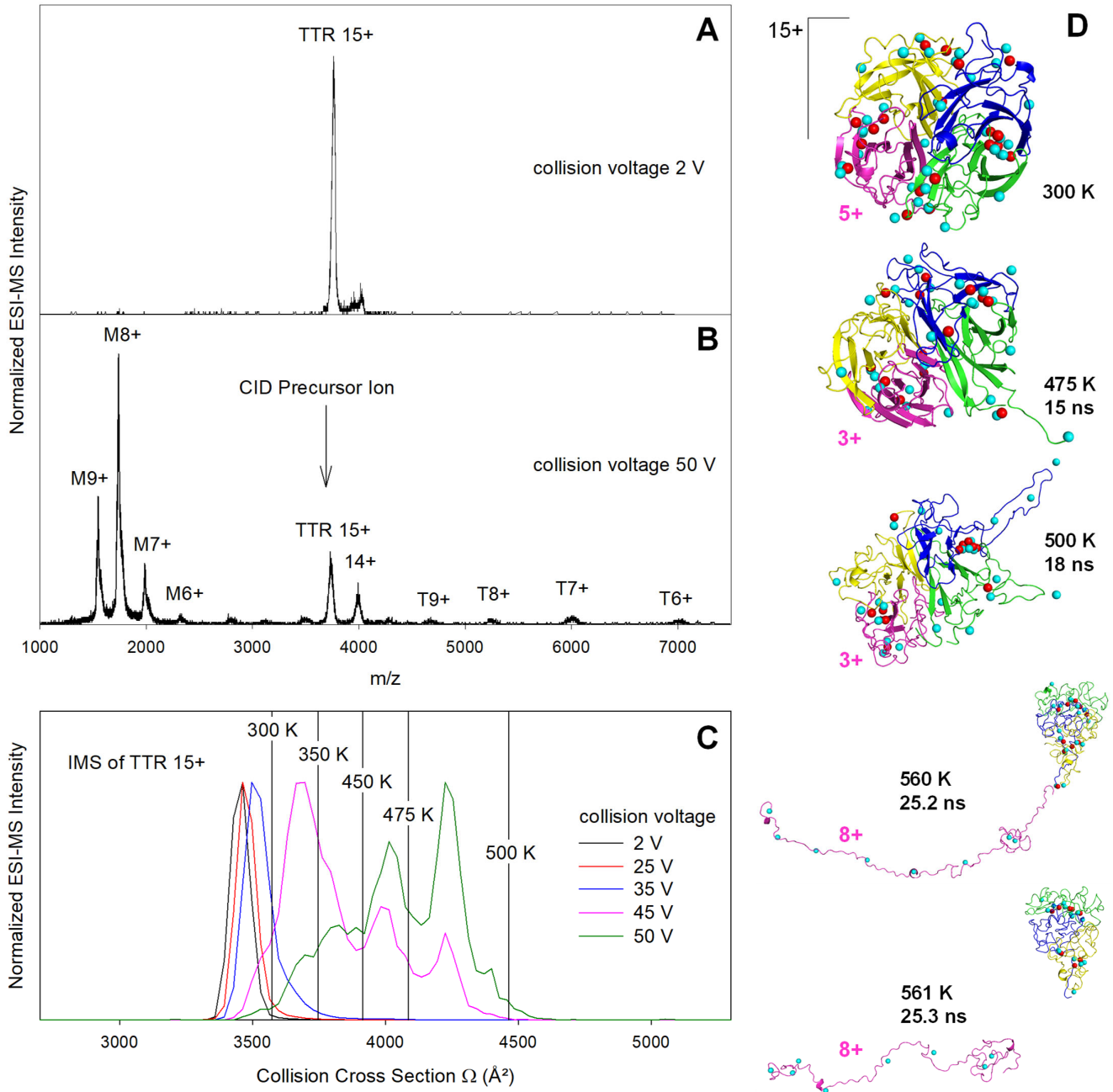
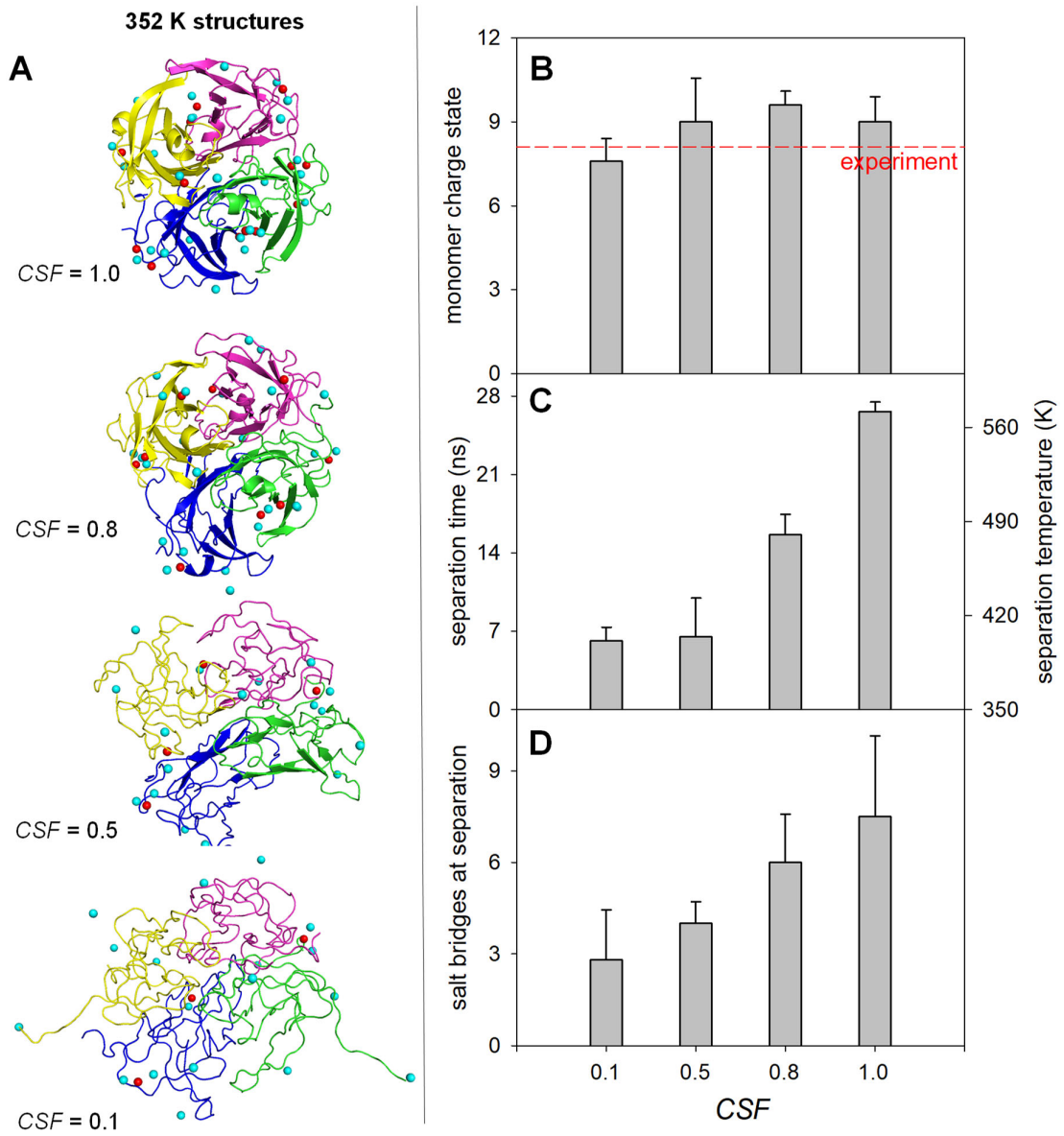
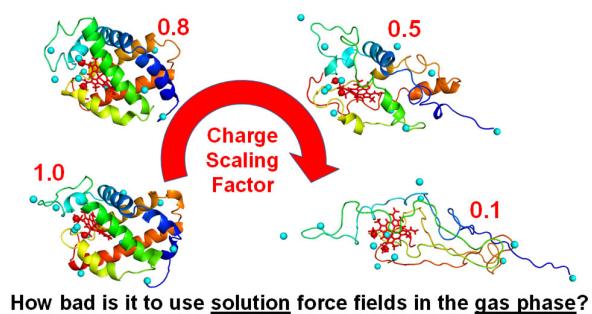


Figure 6



TOC Graphic



How bad is it to use solution force fields in the gas phase?

[TOC Graphic was pasted into the .docx document as device-independent bitmap. If resizing is required, please drag the bottom right corner.]